IEEE Access
Multidisciplinary | Rapid Review | Open Access Journal

Received October 28, 2018, accepted November 18, 2018, date of publication November 26, 2018,
date of current version December 27, 2018.

Digital Object Identifier 10.1109/ACCESS.2018.2883324

Implementation of Optimization-Based Power Management for All-Electric Hybrid Vessels

LIZA W. Y. CHUA[1,2], TEGOEH TJAHJOWIDODO[3], GERALD G. L. SEET[3], AND RICKY CHAN[4]

[1]School of Mechanical and Aerospace Engineering, Nanyang Technological University, Singapore 639798
[2]ABB Pte. Ltd., Singapore 139935
[3]School of Mechanical and Aerospace Engineering, Nanyang Technological University, Singapore 639798
[4]ABB Oy, 00980 Helsinki, Finland

Corresponding author: Tegoeh Tjahjowidodo (TTEGOEH@ntu.edu.sg)

This work was supported in part by the Singapore Economic Development Board and in part by ABB Pte. Ltd.

ABSTRACT The increasing concern in environmental impacts contributed by the shipping industry leads to a growing interest toward incorporating sustainable energy sources to conventional power systems, to reduce fuel consumption and emissions. However, such advance power system architectures tend to face greater challenges in optimal power allocation due to the increased flexibility to split the load among multiple power sources and diversified operations of different vessel types. To address the power management challenges, in this paper, an instantaneous optimization-based approach is proposed for an all-electric hybrid power system, which adopts the equivalent consumption minimization strategy (ECMS). First, the dynamic models of the all-electric hybrid power system are formulated in MATLAB\Simulink and validated on a laboratory-scaled hybrid power system testbed. The power management problem is then formulated using ECMS approach, and a multi-level power management framework is proposed to integrate ECMS solution for practical implementation on an all-electric hybrid vessel. Finally, the feasibility of the proposed approach is validated on a full-scale setup identical to an actual all-electric hybrid vessel with dc distribution in MARINTEK, Trondheim, Norway. The performance of ECMS is also benchmarked against an improve rule-based strategy. The experimental results demonstrated that ECMS can achieve a substantial fuel savings of up to 24.4% as compared with improved rule-based strategy over one cycle of harbor tugboat operations, with the presence of available shore charging.

INDEX TERMS Power management system, energy management, optimization, hybrid power system, energy storage, batteries, marine vehicles.

I. INTRODUCTION

Over the past decades, the maritime industries have been moving towards ship electrification to improve system efficiency, stability and performance. Diesel electric vessels have demonstrated the improvement in fuel efficiency [1], but such vessels are still heavily reliant on marine diesel oil (MDO). With the increasing concern in environmental impacts contributed by the shipping industry, there is a growing interest in the maritime industry towards sustainable energy sources to reduce fuel consumption and greenhouse gases emissions. Over the years, advancements in power electronics have open up the possibilities to include sustainable power sources and energy storage such as batteries, super capacitors, ultra capacitors and fuel cells for maritime applications [2]–[5]. The use of energy storage devices increases the flexibility in power allocation among the power sources, offering the potential to improve fuel efficiency and reduce emission during ship operations. Examples of the uses of batteries include peak shaving and enhanced dynamic support to absorb fast load variations, and strategic loading to allow engines to operate within optimal range to improve fuel efficiency [5]–[7]. Also, batteries can be used in place of engine operation during low loading conditions, achieving zero emission operation. Shore power can be utilized to charge batteries when ships return to harbour, and this energy can be used in the next operation. Using of shore power is cheaper and produce less hazardous emissions. These advanced power system with hybrid power sources have shown to be capable of reducing fuel consumption and emissions by 10% to 35% according to [8].

However, the increase in degree of freedom of control resulted in greater challenge for power management control

to the diversified operations of different vessel types. Naval vessels tend to have short pulsed loads related to weapons utilization and control focuses at maintaining system reliability to handle such pulsed loads. Passenger ferries are usually subjected to low emission and low noise operation requirements. Tugboats have multiple modes of operation, requiring full designed bollard pull power during ship assist, and relatively low power during transit and standby, and may face stricter requirements on vessel emission when operating near urban areas. The diverse operating profiles of these different vessel types makes it difficult to optimize the hybrid power system performance over a single designed operating point or apply a common power management strategy across all vessel types. The conventional rule-based/heuristics techniques currently employed in the industry depends largely on the past experience of the system integrators and operators, while optimal power allocation among the power sources are not guaranteed. Fuel efficiency will not be maximized if power split between the hybrid power sources are not handled properly [9]. Therefore, advanced power management control strategies are necessary to exploit the full potential of the hybrid power system to achieve significant reduction in fuel consumption or emissions [8], [10].

In recent years, power management strategies based on optimization methods are proposed to tackle the power management problem for advanced power and propulsion architectures in the maritime industry. For naval vessels, power management tend to focus on maintaining system reliability, redundancy, and handling of short pulsed loads related to weapons utilization to ensure mission effectiveness. Fuel consumption and emission are of a lower priority in these cases. In [11], sensitivity function method (SFM) is first proposed to improve computational efficiencies of dynamic optimization. Subsequently, it is applied for the power management problem of an Integrated Power System (IPS) of naval vessel in [12] and [13], demonstrating real-time applications. Model Predictive Control (MPC) has been investigated for various marine applications. In [14] and [15], MPC is used to handle fast and sudden pulse loads from weapons operations. In [3], MPC is proposed for electric ships with hybrid energy storage system to mitigate load fluctuations and demonstrates its feasibility in real-time applications. In [16], non-linear MPC (NMPC) is used to control the battery for smoothing of power fluctuations experienced by OSV during dynamic positioning operation. Optimization-based approaches targeted at minimizing fuel consumption are quite limited, and mainly applied for commercial vessels. For example, in [17], static optimization is used to develop a battery charge-discharge mode for a hybrid Offshore Supply Vessel (OSV). The results show fuel savings in comparison to other system architecture, but performance of the proposed technique against rule-based, or other advanced power management strategies are not discussed. QP and Mixed-Integer Programming were investigated in [18], however the results show frequent starting and stopping of generators in simulation study, which is undesirable in real life application. In [19] and [20], Equivalent Consumption Minimization Strategy is first investigated on different hybrid diesel electric vessel layout to investigate the capabilities for fuel reduction. Previous work in [21] and [22] proposed a method with ECMS to optimize engine operations around the optimal operating point, and simulation results on a harbour tugboat case study shows up to 17.6% fuel savings compared to industrial rule-based techniques. Recent studies in [10] proposed an adaptive ECMS (A-ECMS) for hybrid tugboat, showing better performance than rule-based and demonstrates near optimal performances when compared to global optimum solution from DP under simulation. However, these proposed ECMS approaches are executed in simulation-based environments, and have not been demonstrated on an actual full-scale system in real-time.

Hence, this study aims to implement and validate the performance of ECMS in real-time on an actual all-electric hybrid power system, to optimize fuel efficiency. The main contributions of this study include: Firstly, dynamic models of the hybrid power system is formulated and validated on a laboratory-scaled hybrid power system test bed set up in NTU Mechtronics lab, Singapore, that can be used as a platform for initial power management studies and development. Secondly, a multi-level framework is proposed for practical implementation of the ECMS approach proposed in earlier work [21] and [22], on the actual hybrid power system. Preliminary investigations to validate the feasibility of the proposed framework is performed on the laboratory-scaled test bed before implementing on actual system. Finally, the proposed framework is validated on an actual system in a laboratory facility with a full-scale hybrid all-electric vessel system layout and industrial control system in MARINTEK, NTNU, Norway. In addition, the performance of ECMS is evaluated against an improved rule-based strategy that set a higher benchmark, to demonstrate the advantages of proposed ECMS approach over conventional rule-based methods.

The rest of the paper is organized as follows: Chapter II describes the modelling and validation of the power system components of an all-electric hybrid power system on a laboratory-scaled test bed. Chapter III introduces the proposed multi-level power management framework and described the supervisory power management strategies. The feasibility of the proposed framework is investigated on the laboratory scale test bed. In Chapter IV, the proposed framework is implemented on a full-scale test bed and results were presented and discussed. Chapter V concludes with a summary of the work and recommendation for future research.

II. ALL-ELECTRIC HYBRID POWER SYSTEM

The schematic of an all-electric hybrid power system is shown in Fig. 1. The main power sources comprises of engine-generators (gensets) and batteries. Vessel loads usually includes the main propulsion load, service and hotel loads such as pumps, Heating, Ventilation and Air-conditioning (HVAC) and lightings. In this study, the system considered

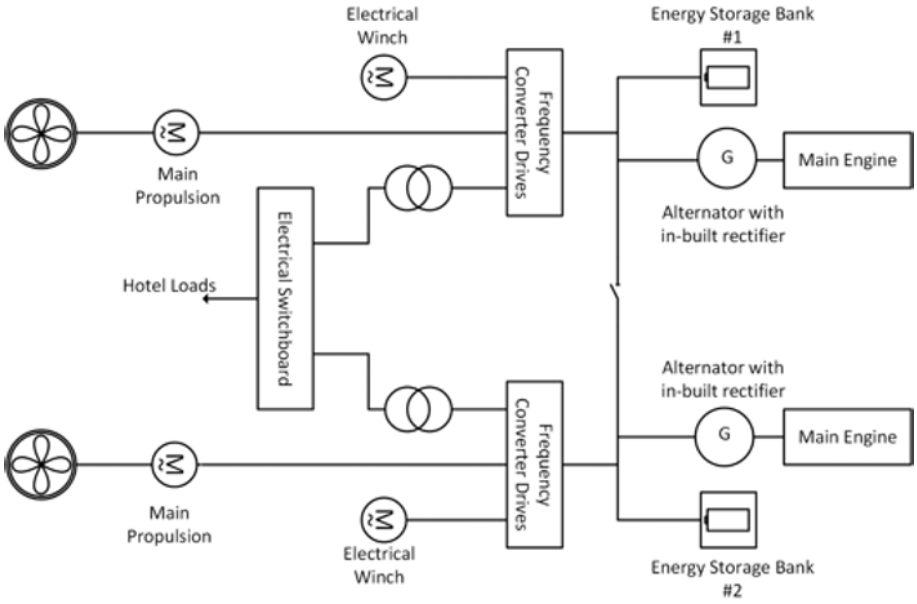

FIGURE 1. All-electric hybrid power and propulsion system.

uses a modern DC distribution system. The main advantages includes the increase in fuel efficiency with the use of variable speed engines in DC power distribution system and easy integration of DC hybrid power sources [23]. Other advantages of using the DC distribution are highlighted in [24]. The AC power from the gensets are converted to DC power through rectifier, while charging and discharging of the battery is controlled by the bi-directional DC-DC converter.

The hybrid power system components are modeled on the MATLAB\Simulink platform to simulate the dynamic responses of the power system. The dynamic response of the models are validated and calibrated against a laboratory-scaled hybrid power system test bed described in this section.

A. LABORATORY-SCALED HYBRID POWER SYSTEM

For preliminary validation of the proposed framework, a laboratory-scaled test setup is used. The laboratory-scaled hybrid power system considers the main power sources and power converters of an all-electric power systems. Due to the space and ventilation constraints to install a full scale diesel engine in this laboratory environment, the diesel engines are emulated by two Permanent Magnet Synchronous Motors (PMSM) driven by a variable frequency inverter as the prime movers. Studies are conducted in the next section to validate that the motors can be representative for the dynamic response of the diesel engine. The schematic of the test bed is as shown in Fig. 2(a), and the actual lab setup is shown in Fig. 2(b). The specifications of the laboratory equipment are listed in Table 1.

The controls of the hybrid power system testbed are implemented by dSPACE DS1103 PPC controller board. The DS1103 PPC Controller Board enables the implementation of a real-time control system with a slave-DSP subsystem based on Texas Instruments TMS320F240 DSP microcontroller [25]. The controller board is connected to a desktop on Windows operating system installed with dSPACE software. The software includes Real-Time Interface (RTI) for code generation, RTI blocksets for MATLAB\Simulink and ControlDesk for real time monitoring and control. To implement the controls, control models are developed on the Simulink platform using RTI blocksets.

TABLE 1. Specifications of laboratory-scaled hybrid power system test bed.

Equipment	Specifications
Permanent Magnet Synchronous Motors (Model: CDQC TP112M-4-E)	4kW, 50Hz, 4 poles, 380V, 8.07A
Brushless synchronous generator (Model: MECC ALTE ECP28-1VS/4A)	7.8kVA, 50Hz, 4 poles, 400V
Li-ion battery module (3 units connected in series)	50.4V, 34.8Ah, 0.2C (maximum continuous charging/discharging)
Bidirectional DC-DC converter	Discharging Voltage control: 0-600V, Power control: 0-4kW (boost) Charging Fixed charging: 1.5kW (buck)
DC load (Resistor bank with 10 solid state relay circuits)	10kW at 540V (Maximum)
Rectifier (3-phase diode bridge rectifier module)	100A, 1600V
DC-link smoothing capacitor (2 units connected in series)	1200μF, 550V

B. MODELING AND VALIDATION OF HYBRID POWER SYSTEM COMPONENTS

1) ENGINE-GENERATOR SET

The diesel engine model has been well established in other studies. The level of complexity of the model depends on

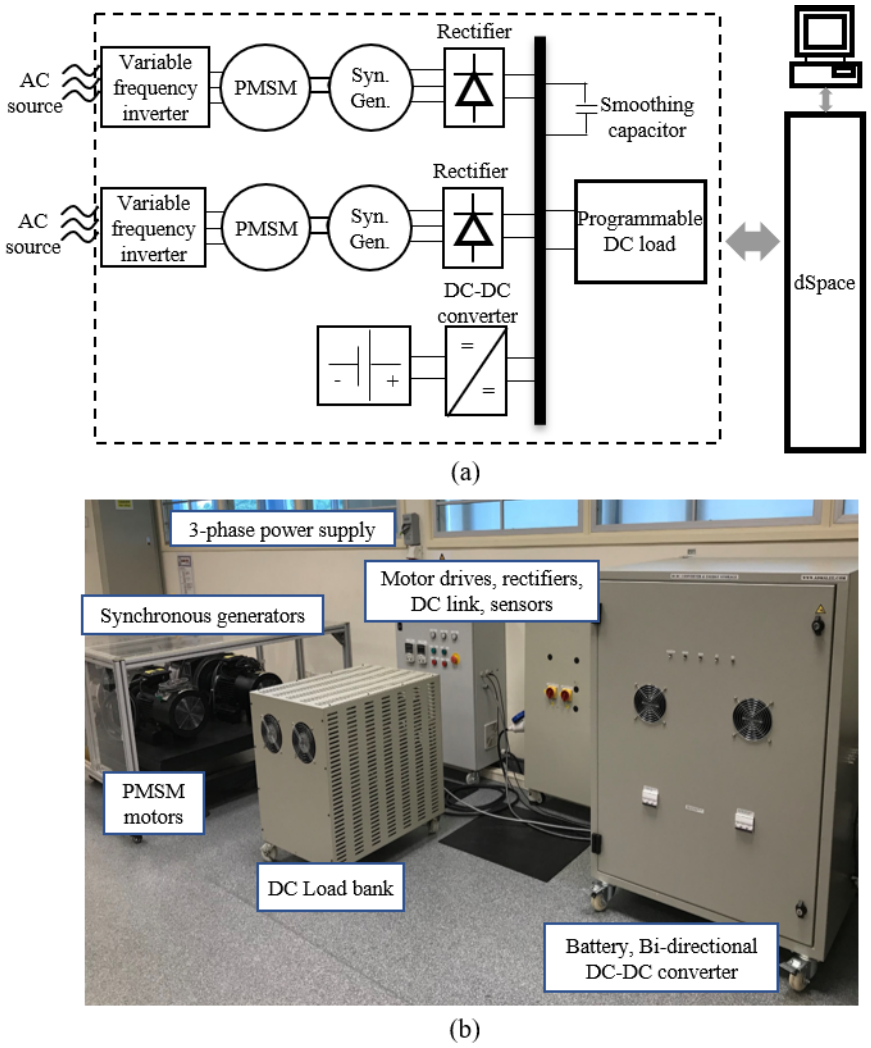

FIGURE 2. Hybrid power system test bed (a) Schematic (b) Laboratory layout.

the application. For power management studies, the engine can be modeled as a first order system with time delay that relates between the fuel injection input and output torque of the engine in terms of per unit (p.u.) as follows [26]:

$$T_m(s) = \exp^{-\tau s} \frac{K_y}{1 + \tau_c s} Y(s) \tag{1}$$

where $T_m(s)$ is the output torque, K_y is the torque constant, and $Y(s)$ is the fuel index expressed in nominal values from 0 to 1.0 p.u.. Since both the output torque and fuel index are expressed in p.u., the torque constant is assumed to be normalized at rated value. The time delay τ and time constant τ_c can be calculated by [26]:

$$\tau \approx \frac{1}{2n_m N} \tag{2}$$

$$\tau_c \approx \frac{0.9}{2\pi n_m} \tag{3}$$

where n_m is the engine rotational speed (rps), and N is the number of engine cylinders. The mechanical system of the engine translates the output torque to angular motion. Using Newton's second law for rotation, the mechanical system can be represented as [27]:

$$J_{eq} \frac{d\omega}{dt} = T_m - T_{em} - \omega_m C_r \tag{4}$$

where J_{eq} is the equivalent inertia of the engine shaft, T_{em} is the electromechanical torque of the synchronous generator, ω_m is the rotational speed of the engine (rad/s) and C_r is the rotational losses coefficient. Using the formulation described in [27], an inertia constant H can be defined to express equation (4) in p.u., where $J_{eq} = 2H$. The engine model parameters are given in Table 2.

The governor is modeled as a PI controller to regulate the engine speed based on a given speed reference. For variable speed engines, the speed references to the governor are adjusted at different engine loading to optimize

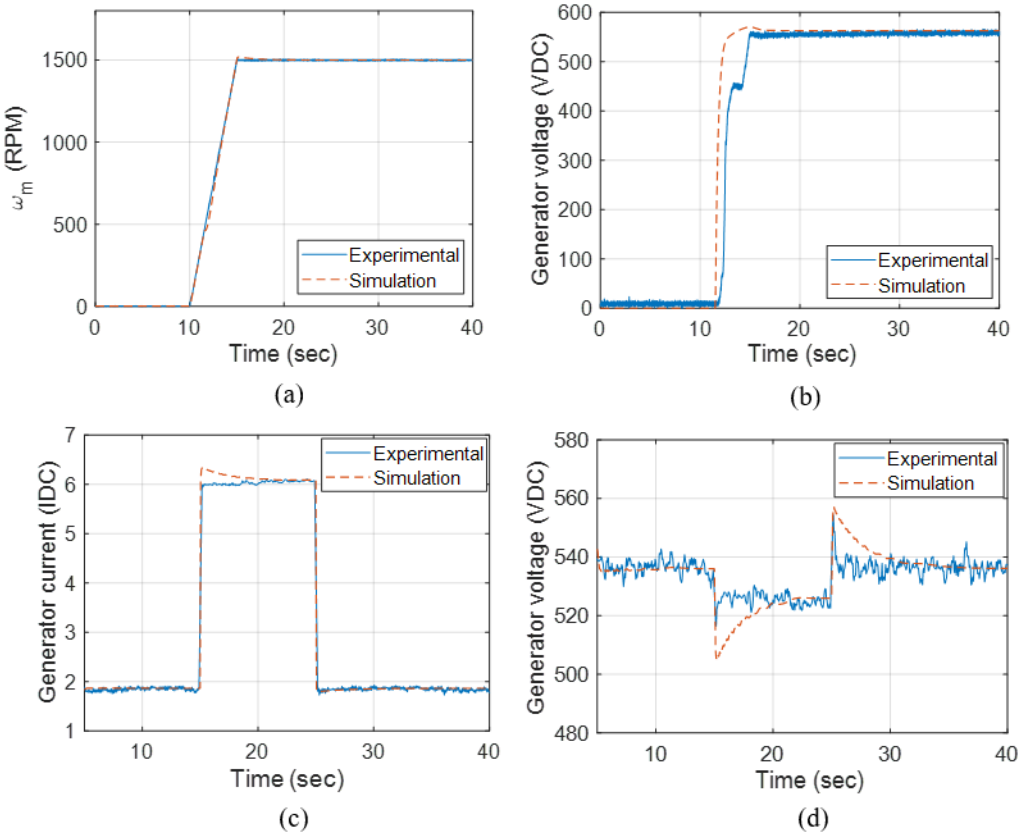

FIGURE 3. (a) Step speed input and (b) Voltage output under no-load condition and (c) Step load input and (d) Voltage output under step-load condition.

TABLE 2. Engine Model Parameters.

Parameters	K_y	N	H	C_r	n_m
Values	1.0	6	0.26	0.01289	25

fuel efficiency. Based on the Specific Fuel Oil Consumption (SFOC) map of the diesel engine given by the engine manufacturers, speed reference at each engine loading can be derived and implemented using a lookup table. The synchronous generator model in per unit system is adapted from the MATLAB\Simulink Simscape Power System library. The model takes exciter field voltage and engine rotational speed as input to generate three phase AC voltage on the output. The excitation system regulates the output voltage of the generator by adjusting the field voltage through the automatic voltage regulator (AVR) and exciter. The AVR is modeled as a PI controller and a first order system is used to represent the exciter. The three phase AC voltage output from the generator is converted to DC voltage on the main power distribution line through a rectifier.

The dynamic response of the actual motor-generator set and simulated engine-generator model is investigated under both loaded and unloaded conditions. Under the unloaded condition, a step input from zero to rated speed is applied to the prime mover at no load, and the generator rotation speed and no load voltage after the uncontrolled rectifier output is measured. The generator rotation speed response of both the actual motor-generator set and simulated engine-generator model follows the same ramp rate under step input, as shown in 3 (a). Comparing the generator output voltage response, the simulation model assumes an ideal condition where the P and I parameters of the AVR are fine tuned to achieve close to a critically damped response as shown in Fig. 3 (b). In actual experimental setup, the P and I parameters of the AVR are fixed at its default values in this case, reflecting the difference in damping response against the ideal case in simulation. Regardless of the slight difference of the damping response, the simulation model shows close relation to experimental results in terms of transient rise time, as well as the steady-state generator output voltage. A step load is then applied to the generator at rated speed as shown in Fig.3 (c), to simulate the voltage droop of the generator across the rectifier. As the AVR attached to the generator in this test bed is not configured to receive voltage reference from external controls, the generator droop on the test bed could not be adjusted. Instead, the voltage setpoint on the generator model is adjusted to match the experimental results as shown in Fig. 3 (d).

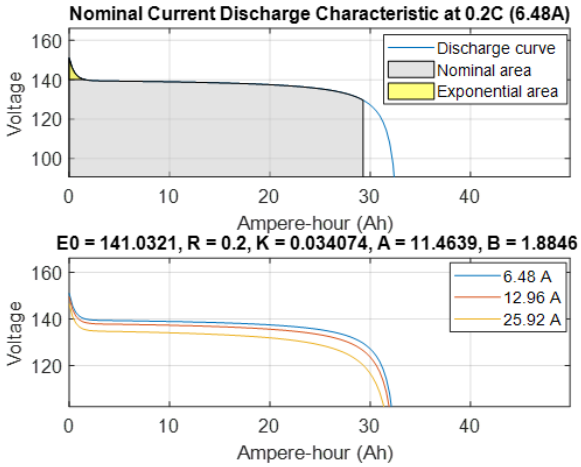

FIGURE 4. Battery discharge characteristics.

2) ENERGY STORAGE SYSTEM

The energy storage system comprises of Li-ion battery and the bidirectional DC-DC converter. A generic Li-ion battery model is implemented from the MATLAB\Simulink Simscape Power System library where battery voltage for the charging and discharging mode is defined as [28]:
When $i^* < 0$,

$$E_{charge} = E_0 - \frac{K \cdot Q}{it + 0.1 \cdot Q} \cdot i^* - \frac{K \cdot Q}{Q - it} \cdot it + A \cdot \exp(-B.it) \tag{5}$$

When $i^* > 0$,

$$E_{discharge} = E_0 - \frac{K \cdot Q}{Q - it} \cdot i^* - \frac{K \cdot Q}{Q - it} \cdot it + A \cdot \exp(-B.it) \tag{6}$$

where E_{charge} and $E_{discharge}$ are the battery charge and discharge voltage (V) respectively. E_0 is battery constant voltage (V), K is the polarization constant (Ah^{-1}), Q is the maximum battery capacity (Ah), i^* is the low frequency current dynamics (Amphere) and it is the extracted capacity (Ah), which can be derived from $it = \int idt$. A is exponential voltage (V) and B is the exponential capacity (Ah^{-1}), which can be obtained from the battery discharge characteristics curve are shown in Fig. 4. The temperature and aging effects of the battery are not considered.

The bidirectional DC-DC converter, as shown in Fig, 5, is necessary for the voltage and current control of the battery. In the buck mode, $S2$ is active, and $S1$ acts as a diode, stepping down the voltage and allow battery to charge. In the boost mode, $S1$ is active, and $S2$ acts as a diode, stepping up voltage output at V_{DC}, enabling battery to discharge. An average value model of the converter with current and voltage control loops adapted from [29] is implemented in this study, where the switch model is replaced with current/voltage sources as shown in Fig. 6(a) and (b). The converter is assumed to be working in a continuous operation mode. The design parameters of the converter are listed in Table 3. A charging and

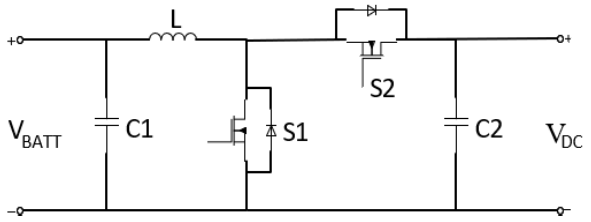

FIGURE 5. Bidirectional dc-dc converter.

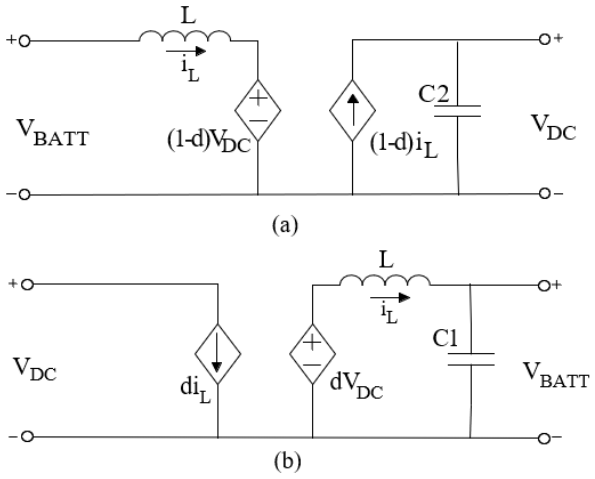

FIGURE 6. Average value model (a) Boost (b) Buck.

TABLE 3. Bidirectional DC-DC converter parameters.

Parameters	L	$C1$	$C2$
Values	$9.152mH$	$500\mu F$	$1200\mu F$

discharging cycle is applied to compare the response between the average value model and actual converters, as shown in Fig. 7. The converter is operated in voltage control mode throughout. V_{batt} and I_{batt} are measured at the output of the battery modules, and VDC and IDC are measured at the output of the bi-directional dc-dc converter. The simulation models assumes ideal condition where there is no losses across the bi-directional dc-dc converter. Hence in experimental results, due to the losses across the converter during discharge, it is observed that battery discharge higher current to achieve the same output current at the converter, as shown in Fig. 7 (c) and 7 (d). Similarly for charging, current flowing into the battery is lower in experimental results than in simulation, although converter demands slightly more current from the grid. Comparing the voltage trends in Fig. 7 (a), V_{batt} slightly differs between experimental and simulations as a result of the different in battery current during charging and discharging. Comparing the output voltage in 7 (b), converter reference voltage is set at 540Vdc for both simulation and experiments. The converter works well in maintaining output voltage at reference voltage of 540Vdc through fine tunning PI controllers in simulation. While in experiments, the converter controller has an accuracy of 5% for voltage control, resulting in slightly lower output voltage. In addition,

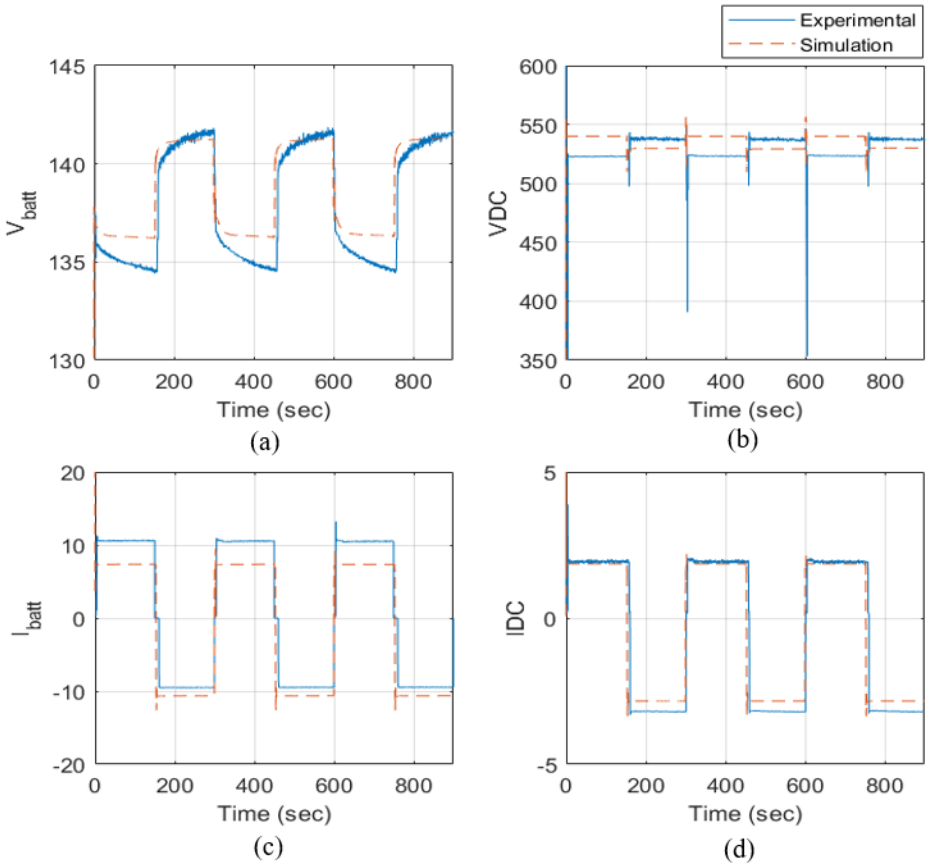

FIGURE 7. (a) Battery and (b) Bidirectional DC-DC converter output voltage, (c) Battery and (d) Bidirectional DC-DC converter output current.

a few instances of large voltages dips are observed when battery changes from charging to discharging. This is due to a constraint in the construction of the converter device where there is a lag-time to switch between the charging and discharging circuit. Due to such limitations in experimental setup, there were rare instances of the sudden mismatch between power supply and demand, resulting in large voltage dip in 7 (b). For example at $t = 600$, generator 1 received switch off command, while the battery did not discharge immediately due to the lag-time in switching circuit, leading to the insufficient power supply to meet the power demand. However, the system was able to recover and continue operation. In the simulation and in real life application on actual system, the DC-DC converters are not subjected to such limitation and therefore such performance is not expected.

Overall, the dynamic models are validated and calibrated against the laboratory-scale test bed, and close dynamic response between the simulation and experimental results are shown in Fig. 3 and Fig. 7 for the gensets and batteries respectively. The validated models can be easily reconfigured for different system configurations based on the number of gensets and batteries modules in the vessel design, for future studies and development of power management strategies.

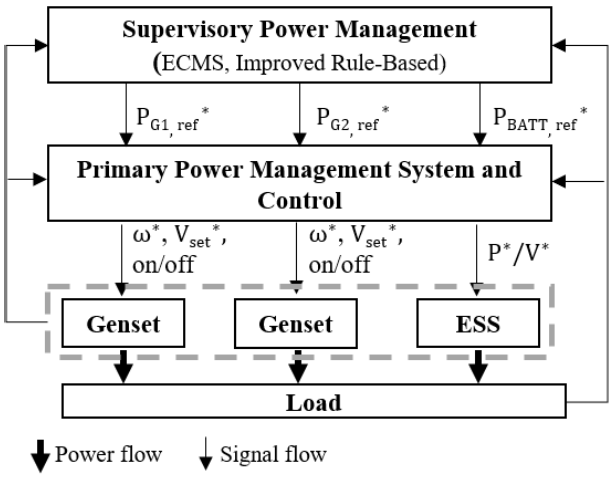

FIGURE 8. Multi-level power management framework.

III. MULTI-LEVEL POWER MANAGEMENT FRAMEWORK

A multi-level power management framework is proposed, as shown in Fig. 8, to integrate the advanced power management strategies using optimization-based methods to existing power management control of the system.

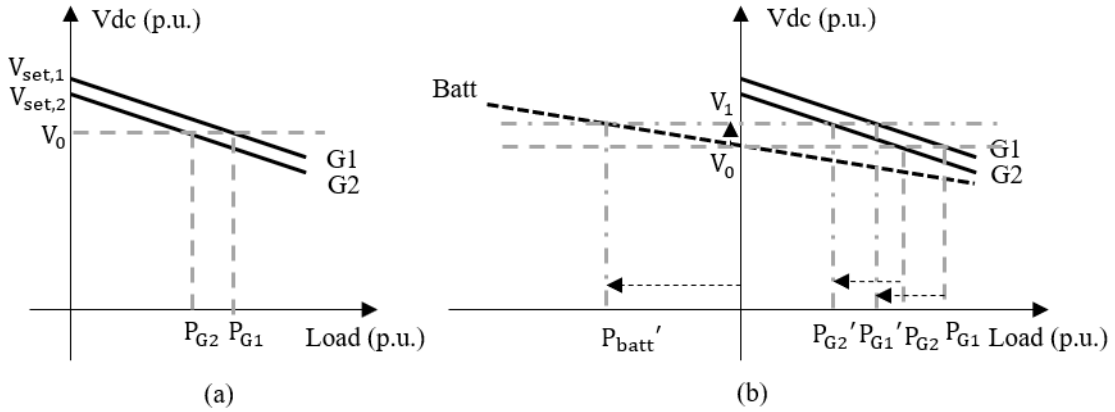

FIGURE 9. Voltage droop characteristics of (a) Two Generators (b) Two Generators with battery.

A. PRIMARY POWER MANAGEMENT SYSTEM AND CONTROL

The primary functions of the power management control of ship power and propulsion system includes voltage and frequency control to maintain the stability of distribution line, manage load sharing among the power generation sources as well as load distribution among the consumers, protection control and blackout preventions. In the DC power distribution system, the balance of power generation and consumption is achieved through voltage droop control. When two or more generators are in parallel, the load sharing among the generators depends on the droop characteristic of the generator as shown in Fig. 9(a). At DC grid voltage V_0, the generators share the load at P_{G1} and P_{G2} according to their respective droop. Equal load sharing can be achieved if the generators have equal droop, which can be achieved by adjusting the voltage setpoints $V_{set,1}$, $V_{set,2}$, and their droop settings. Conventionally, the number of generators online are decided based on load dependent start/stop rules. In pure mechanical or diesel-electric power system where diesel generators are the only type of power source, optimizing the number of generators online to achieve greater fuel efficiency can be straight forward by formulating the load dependent start/stop rules from static optimization results based on engine SFOC data [30].

In hybrid DC power system with battery, droop control can also be implemented to control the load sharing between the hybrid power sources [31]. The voltage droop concept is illustrated in Fig. 9(b). At the initial voltage V_0, battery supplies zero power, while generator 1 and 2 shares the load at P_{G1} and P_{G2} respectively. When there is a sudden reduction in load, the excessive power in the system is first absorbed by the battery P'_{batt}. As battery voltage setpoint increases from V_0 to V_1, generator 1 and 2 decreases their load to P'_{G1} and P'_{G2} following the droop curve and power absorbed by the battery gradually reduces to zero. However, it can be observed that the utilization of battery power largely depends on the droop settings and adjustments, which may not exploit the full potential of the hybrid sources to achieve fuel efficiency.

In recent years, advanced power management control strategies are investigated. One of these methods is to formulate the power management problem into an optimization problem, where the optimal power split between the multiple power sources are determined through numerical methods.

B. EQUIVALENT CONSUMPTION MINIMIZATION STRATEGY

The formation of a power management problem into an optimization problem requires each decision variable to have an associated cost, and this cost has a direct impact on their optimal value while solving the cost function. However, in the case of an all-electric hybrid power system, it is clearly recognizable that the cost of battery energy is not directly comparable to the energy cost of fuel. In [32], the concept of Equivalent Consumption Minimization Strategy (ECMS) was first introduced in automobile applications as a solution to this problem. ECMS is developed based on the assumption that the amount of battery energy used will be recharged by the engines in the future. Hence, an equivalent fuel cost for battery energy can be derived by considering the average fuel required to charge the battery along the energy path from the engine to the battery. ECMS considers only instantenous equivalent fuel cost, and hence it is real-time implementable. Although this approach does not give global optimal solutions by minimizing fuel consumption over the whole operating profile, earlier works in [21] and [22] have proposed an ECMS approach which demonstrates promising fuel savings over rule-based strategy for an all-electric hybrid vessel through simulation, over a case study on a harbor tugboat operation. ECMS approach proposed in [10] have also shown near optimal results.

In this study, the main control objective of the power management strategy is to minimize fuel consumption. Extending from proposed ECMS approach in [21] and [22], the cost function is formulated as:

$$\min J = \sum_{i=1}^{n} C_{eng,i} + C_{batt,eqv} = C_{total,eqv} \tag{7}$$

where $C_{total,eqv}$ (g/s) is the total equivalent consumption, $\sum_{i=1}^{n} C_{eng,i}$ (g/s) is the total fuel consumption from n engines, and $C_{batt,eqv}$ (g/s) is the equivalent fuel consumption of the batteries. The fuel consumption of the each engine can be obtained as:

$$C_{eng,i} = SFOC(P_{gen,i}) \cdot \frac{P_{gen,i}}{n_{gen,i} \cdot 3600} \tag{8}$$

As proposed in previous work [21], the equivalent fuel consumption of the batteries can be expressed as:

$$C_{batt} = FC \cdot \frac{P_{batt}}{n_{gen,i} \cdot n_{batt} \cdot 3600} \tag{9}$$

where $SFOC(P_{gen,i})$ is the specific fuel oil consumption at the engine loading (g/kWh), $P_{gen,i}$ is power delivered by the engine (kW), P_{batt} is the power delivered by the battery (kW), $n_{gen,i}$ and n_{batt} are the efficiencies of the generator and battery respectively. FC is the fuel consumption conversion factor, which is a critical factor that defines how the equivalent cost of the battery is formulated. FC is proposed to be set at the minimum $SFOC$ value of the engine in [21] and [22], which can maximize engine's operation around the optimal loading point. The cost function is subjected to linear and non-linear equality constraints to ensure that load demand is met, as well as inequality constraints due to the system limitations stated as follows:

$$P_{gen,imin} \leq P_{gen,i} \leq P_{gen,imax} \tag{10}$$

$$-P_{battmin} \leq P_{batt} \leq P_{battmax} \tag{11}$$

$$SOC_{min} \leq SOC \leq SOC_{max} \tag{12}$$

where $P_{gen,imin}$ and $P_{gen,imax}$ are the minimum and maximum power rating of the ith genset, $P_{battmin}$ and $P_{battmax}$ are the charging and discharging limits of the battery, and SOC_{min} and SOC_{max} are the minimum and maximum SOC limits of the battery respectively.

A few assumptions were taken in the problem formulation. Firstly, the power management problem considers the fuel consumption at steady-state values and hence, fuel consumption during engine ramping is not considered. Secondly, the losses through engine-generator coupling, propulsion drive-trains, as well as efficiencies of the battery during charging/discharging and bi-directional DC-DC converter are assumed to be constant. This method does not require prior knowledge of the load demand, hence making it straight forward for real-time implementation. The instantaneous cost function is solved with non-linear constrained optimization solver using interior point method in MATLAB.

C. IMPROVED RULE-BASED STRATEGY

The effectiveness of ECMS over conventional and industrial available rule-based (RB) controller has been proven in previous works [10], [21], [22], where ECMS strategy can demonstrate up to 17.8% fuels savings. With the understanding and knowledge gained from the solutions of optimization-based strategies, RB strategies can be improved. Therefore in this study, an improved RB strategy is formulated by utilizing the information from the optimized solution on the same operation profile in previous works to formulate the operation rules. The operation rules are pre-defined based on load level and battery SOC condition to determine the power allocation. The introduction of an improved rule-based strategy in this work aims to set a higher benchmark to further evaluate the advantages of the proposed strategy against rule-based methods. For the same system consisting of two gensets and batteries as main power sources, the cases of operation generated by the refined operation rules are illustrated in Table 4.

D. PROPOSED FRAMEWORK

In the proposed framework as shown in Fig. 8, the primary level represents existing fundamental power management control in the system, where voltage droop functionalities, load dependent start/stop rules and protection controls are executed. This level also takes care of the main communications and control between the drives, field controllers and the power system components. ECMS and improved rule-based strategy are implemented on the supervisory level. At every time step, the optimal power split between the power sources are determined from the power management strategies.

The power references from the supervisory level are implemented through the existing fundamental power management control of the power system by manipulating the on/off control of the genset, and controlling the battery charging/discharging power through the bi-directional dc-dc converter in power and voltage control mode. For gensets, the on/off control is dependent on $P^*_{Gi,ref}$, which represent the power reference values of the ith genset. When $P^*_{Gi,ref} < 0$, the ith genset is offline. When $P^*_{Gi,ref} > 0$, the ith genset will be switched on, and primary level controls will determine the ω^* and V^*_{set} values of the genset. When more than one genset are operating in parallel, the gensets will share the load according to voltage droop control. For battery, charging and discharging controls depend on the battery reference values, $P^*_{BATT,ref}$. When $P^*_{BATT,ref} \geq 0$, battery is in discharging mode. If battery is the only source of power and no gensets in the system are online, DC-DC converter will be in voltage control mode to maintain stable DC grid voltage at V^*. The amount of discharging battery power will be based on the current drawn by the load demand, which should also coincides with $P^*_{BATT,ref}$ generated from supervisory control. When $P^*_{Gi,ref} > 0$ and $P^*_{BATT,ref} \geq 0$, ith genset is online and DC grid voltage will be maintained by ith genset. In this case, the DC-DC converter will operate in power control mode according to battery power reference $P* = P^*_{BATT,ref}$. Since battery discharging power is controlled at $P^*_{BATT,ref}$, the genset will deliver the remaining required power of the load demand. Finally, when $P^*_{BATT,ref} < 0$, the converter will switch into charging mode, demanding $P^*_{BATT,ref}$ from other power sources in the system.

The proposed framework is causal, since both ECMS and improved rule-based strategies does not require future load

TABLE 4. Improved Rule-Based Strategy for a case of all-electric hybrid power system consisting of two gensets and battery.

Power \ SOC	$SOC \leq SOC_{min}$	$SOC_{min} < SOC \leq SOC_{max}$	$SOC \geq SOC_{max}$
$P_{load} \leq P_{G1,on}$	$P_{G1} = P_{G1,opt}, P_{G2} = 0$ $P_{batt} = P_{load} - P_{G1}$ if $P_{batt} > P_{charge,max}$ $P_{batt} = P_{charge,max}$ $P_{G1} = P_{load} - P_{batt}$ end	$P_{G1} = 0, P_{G2} = 0$ $P_{batt} = P_{load}$ if $P_{batt} > P_{discharge,max}$ $P_{batt} = P_{discharge,max}$ $P_{G1} = P_{load} - P_{batt}$ end	$P_{G1} = 0, P_{G2} = 0$ $P_{batt} = P_{load}$ if $P_{batt} > P_{discharge,max}$ $P_{batt} = P_{discharge,max}$ $P_{G1} = P_{load} - P_{batt}$ end
$P_{G1,on} < P_{load} \leq P_{G1,opt}$	$P_{G1} = P_{G1,opt}, P_{G2} = 0$ $P_{batt} = P_{load} - P_{G1}$ if $P_{batt} > P_{charge,max}$ $P_{batt} = P_{charge,max}$ $P_{G1} = P_{load} - P_{batt}$ end	$P_{G1} = P_{G1,opt}, P_{G2} = 0$ $P_{batt} = P_{load} - P_{G1}$ if $P_{batt} > P_{charge,max}$ $P_{batt} = P_{charge,max}$ $P_{G1} = P_{load} - P_{batt}$ end	$P_{G1} = P_{load}, P_{G2} = 0, P_{batt} = 0$
$P_{G1,opt} < P_{load} < P_{G1,opt} + P_{G2,opt}$	$P_{G1} = P_{G1,opt}, P_{G2} = P_{G2,opt}$ $P_{batt} = P_{load} - P_{G1} - P_{G2}$ if $P_{batt} > P_{charge,max}$ $P_{batt} = P_{charge,max}$ $P_{G1} = P_{G1,opt}$ $P_{G2} = P_{load} - P_{G1} - P_{batt}$ end	$P_{G1} = P_{G1,opt}, P_{G2} = P_{G2,opt}$ $P_{batt} = P_{load} - P_{G1} - P_{G2}$ if $P_{batt} > P_{charge,max}$ $P_{batt} = P_{charge,max}$ $P_{G1} = P_{G1,opt}$ $P_{G2} = P_{load} - P_{G1} - P_{batt}$ end	$P_{G1} = \frac{P_{load}}{2}, P_{G2} = \frac{P_{load}}{2}$ $P_{batt} = 0$
$P_{load} \geq P_{G1,opt} + P_{G2,opt}$	$P_{G1} = \frac{P_{load}}{2}, P_{G2} = \frac{P_{load}}{2}$ $P_{batt} = 0$	$P_{G1} = P_{G1,opt}, P_{G2} = P_{G2,opt}$ $P_{batt} = P_{load} - P_{G1} - P_{G2}$ if $P_{batt} > P_{discharge,max}$ $P_{batt} = P_{discharge,max}$ end	$P_{G1} = P_{G1,opt}, P_{G2} = P_{G2,opt}$ $P_{batt} = P_{load} - P_{G1} - P_{G2}$ if $P_{batt} > P_{discharge,max}$ $P_{batt} = P_{discharge,max}$ end

$\mathbf{P_{G1}}$: Power reference of genset 1 from supervisory level (kW), $\mathbf{P_{G2}}$: Power reference of genset 2 from supervisory level (kW), $\mathbf{P_{G1,on}}$: Power setpoint to switch on genset 1 (kW), $\mathbf{P_{G2,on}}$: Power setpoint to switch on genset 2 (kW), $\mathbf{P_{G1,opt}}$: Optimal operating power setpoint for genset 1 (kW), $\mathbf{P_{G2,opt}}$: Optimal operating power setpoint for genset 2 (kW), $\mathbf{P_{load}}$: Load demand (kW), $\mathbf{P_{charge,max}}$: Maximum battery charging limit (kW), $\mathbf{P_{discharge,max}}$: Maximum battery discharging limit (kW)

information, and hence, it can be readily implemented on the test bed in real-time. For real-time implementation, ECMS is solved at load interval of 0.125% and SOC interval at 1% and stored in a lookup table for each power sources. The performance of the proposed power management framework is investigated through a case study on a harbor tugboat operations.

E. CASE STUDY

1) SYSTEM DESCRIPTION

In this case study, the operation of a 60-65BPT harbor tugboat consisting of two gensets and batteries is considered. The main modes of operations can be broadly categorized as *(i) transit*, *(ii) standby or idle*, and *(iii) ship assist* operation. A representative and scaled down time-domain load profile of the harbor tugs derived based on field engine data and experiences of tug owners is obtained from [22] and used in this case study. The duration of the operation cycle is reduced by ten times for the feasibility of laboratory test-bed validation. In this study, 100% loading corresponds to 80% of the total installed generator power of the system. The detailed breakdown of the operation and the scaled duration is shown in Table 5, and the respective time-domain load profile is shown in Fig. 10. The system parameters are following

TABLE 5. Harbor tug operation mode and respective duration.

Operation	Duration (sec)
Standby	36
Transit	108
Standby	180
Transit (follow ship)	72
Standby	30
Ship Assist	18
Standby	24
Ship Assist	18
Ship Assist	24
Ship Assist	18
Standby	72
Transit (return to Port)	120

the specifications of the laboratory-scaled testbed components listed in Chapter II. The proposed power management framework is implemented on the simulation models, before real-time execution on the laboratory scaled hybrid power system test bed. The simulation and experimental results are presented in Fig. 11, 12 and 13.

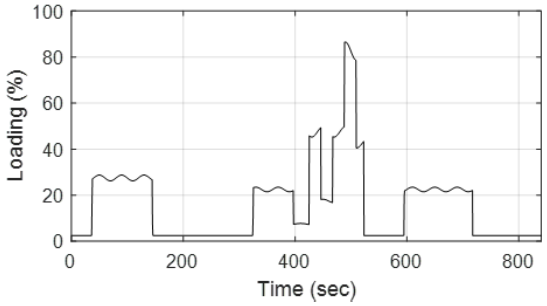

FIGURE 10. Harbor tug time-domain load profile.

2) RESULTS AND DISCUSSIONS

In Fig. 11(a) and (b), it is shown that the steady state voltages on the DC distribution grid is well maintained between 510-550VDC, within 6% of voltage droop, when the proposed framework is implemented with both ECMS and improved rule-based strategy. In simulation, the maximum voltage peaks and dips falls within the acceptable range of 10% throughout the operation cycle. During experiments, a few instances of large voltages dips are observed due to the switching lag-time between the charging and discharging circuit as explained in earlier chapters. The system manage to recover to normal operation after the voltage dips. In Fig. 12 and 13, both simulation and experiment results show that the actual power delivered by the generator and battery closely follows the ideal power references from the supervisory level, which demonstrates the intended performance of the proposed framework. In terms of the performance of ECMS as shown in Fig. 12, both genset 1 and 2 are maintained near optimal operating point of about 60%-80% loading when switched on. During transiting mode, battery operates in charging mode to increase the engine load to improve fuel efficiency. Genset 2 is switched on during the ship assist operation where load demand is high, and shares the load equally with genset 1.

Comparing the fuel efficiency of both strategies, the improved rule-based strategy demonstrates similar performance as the ECMS solution, as shown in Fig. 13. Since power allocation follows similar trends for both strategies, the total fuel consumption under each strategy is similar. Although the total fuel consumption of proposed ECMS is similar to the improved rule-based strategy, this result is expected as the improved rule-based strategy is formulated using the knowledge of optimal power split operating trends from the results in previous works. Apart from fuel efficiency, ECMS approach has added advantages over RB strategies that can be observed from this preliminary validation. Firstly, the improved rule-based strategy works according to pre-defined rules for each loading scenerio. In this case, the improved rule-based strategy has 12 predefined scenarios, as illustrated in Table 4. It can be expected that the number of scenarios and complexity of designing the rule-based logic will increase with additional power sources. Whereas for ECMS, the formulation can cater to n number

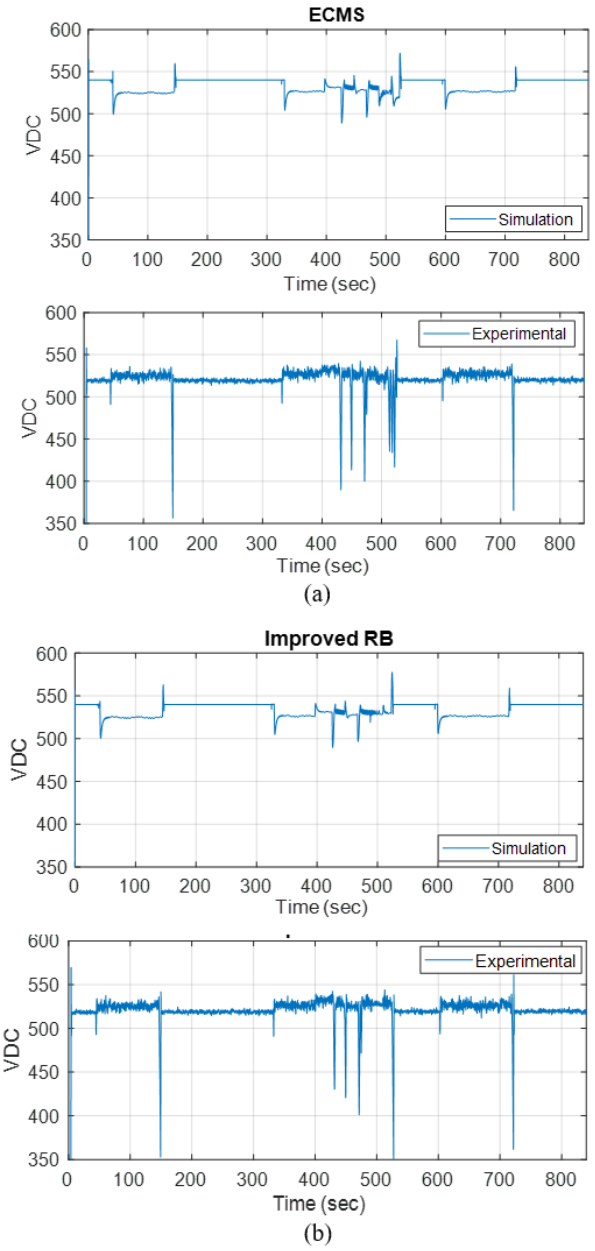

FIGURE 11. Simulation and experimental results of voltage stability for (a) ECMS approach (b) Improved rule-based approach.

of gensets, which is easily adaptable to different system configurations where more power sources are considered. In addition, the solution of the ECMS are generated based on numerical methods to minimize fuel consumption, which can achieve close to optimal results. Whereas, the performance of the rule-based strategy also largely depends on the decision factors such as $P_{G1,on}$, $P_{G2,on}$, $P_{G1,opt}$,$P_{G2,opt}$, which are decided based on experience. Hence, rule-based strategy may not cannot guarantee optimal performance as the ECMS when system parameters or loading scenarios changes.

Overall, from the results shown, the feasibility of the proposed framework is well demonstrated. Experimental results shows that the ideal power references from proposed

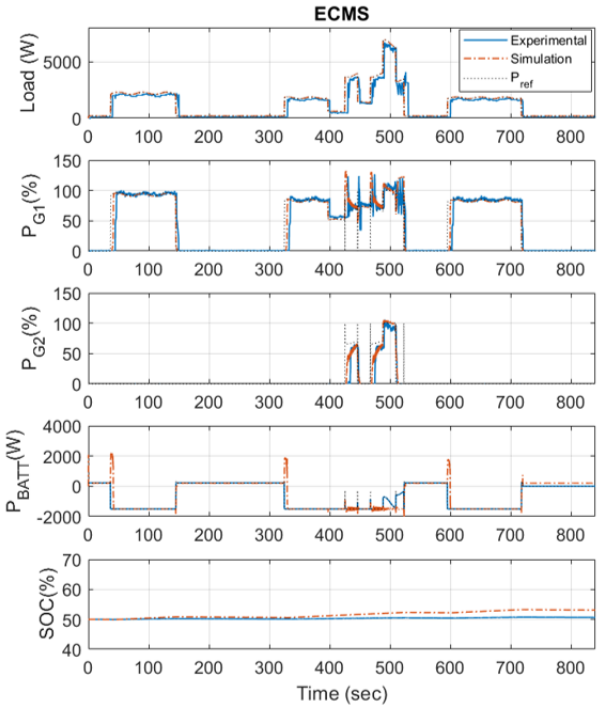

FIGURE 12. Simulation and experimental results with ECMS approach.

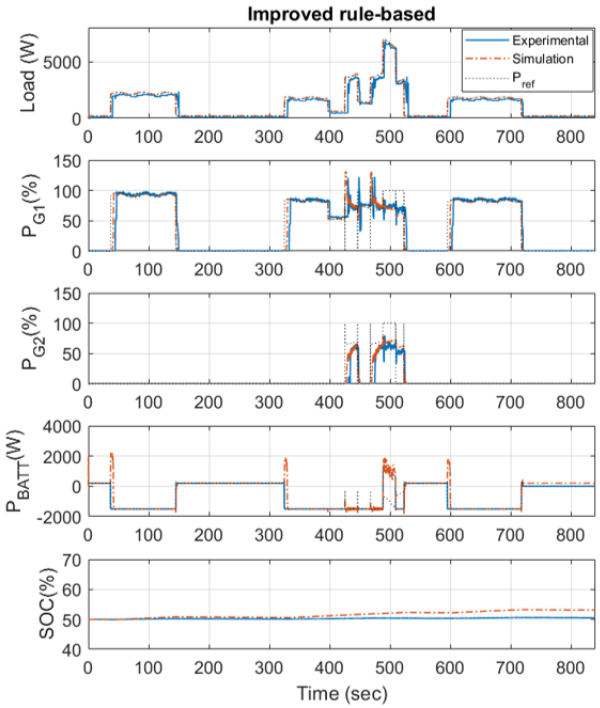

FIGURE 13. Simulation and experimental results with improved rule-based approach.

ECMS on the supervisory level can be executed in real-time. The case study also further validated the simulation model of the hybrid power system described in Chapter II. Similar transient and steady state responses are observed between the simulation and experimental results with both improved rule-based and ECMS. Hence, the simulation model of the hybrid power system can be used as the platform for preliminary studies on further developments of the power management strategies before real-time execution on actual system, or in cases where real-time experiments are not possible. The advantages of proposed ECMS over rule-based approach can be further validated in the full-scale experiment describe in the following section.

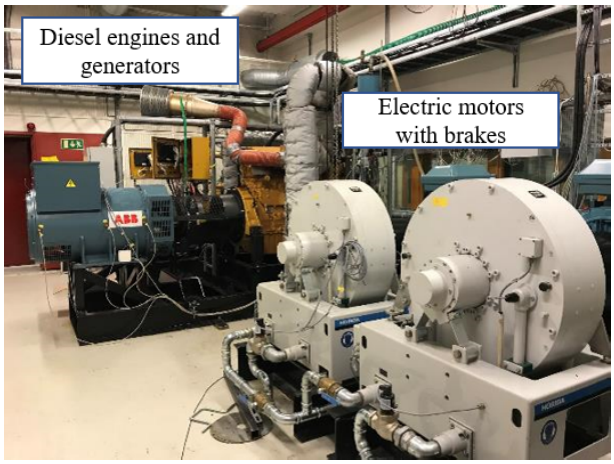

FIGURE 14. Laboratory facilities in MARINTEK.

IV. FULL-SCALE EXPERIMENTAL VALIDATION

With the feasibility of the proposed framework demonstrated on the laboratory-scaled hybrid power system testbed, the performance of the proposed framework is further validated on an actual system as shown in Fig. 14. The facility is located at ABB collaborated hybrid power laboratory in MARINTEK, at the Norwegian University of Science and Technology (NTNU), Trondheim.

A. SYSTEM DESCRIPTION

The system layout is designed based on a full-scale hybrid all-electric vessel with Onboard DC Grid. The system comprises of two high speed diesel engines with variable speed generator sets and energy storage system with battery bank and capacitor bank, connected to a DC distribution system. The system has two electric motor connected to an eddy current brakes to simulate loading scenarios of the power system. The lab facility is shown in Fig. 14. The capacitor bank is not used in this study, and the specifications of the rest of the components are extracted from [6], listed in Table 6. The primary power management control of the system is ABB's Power and Energy Management System (PEMS). Similarly, the tugboat case study is investigated in this full-scale experimental validation. The duration for each operation in Fig. 10 is scaled up proportionally, to increase the total operation cycle time to 35 minutes for a closer representation to the duration of actual tugboat operations.

In order to reduce the use of excess diesel fuel during testing, the tug operation cycle of 35 minutes is executed separately in 3 segments, such that each of the segment can be repeated if necessary, without the need to repeat

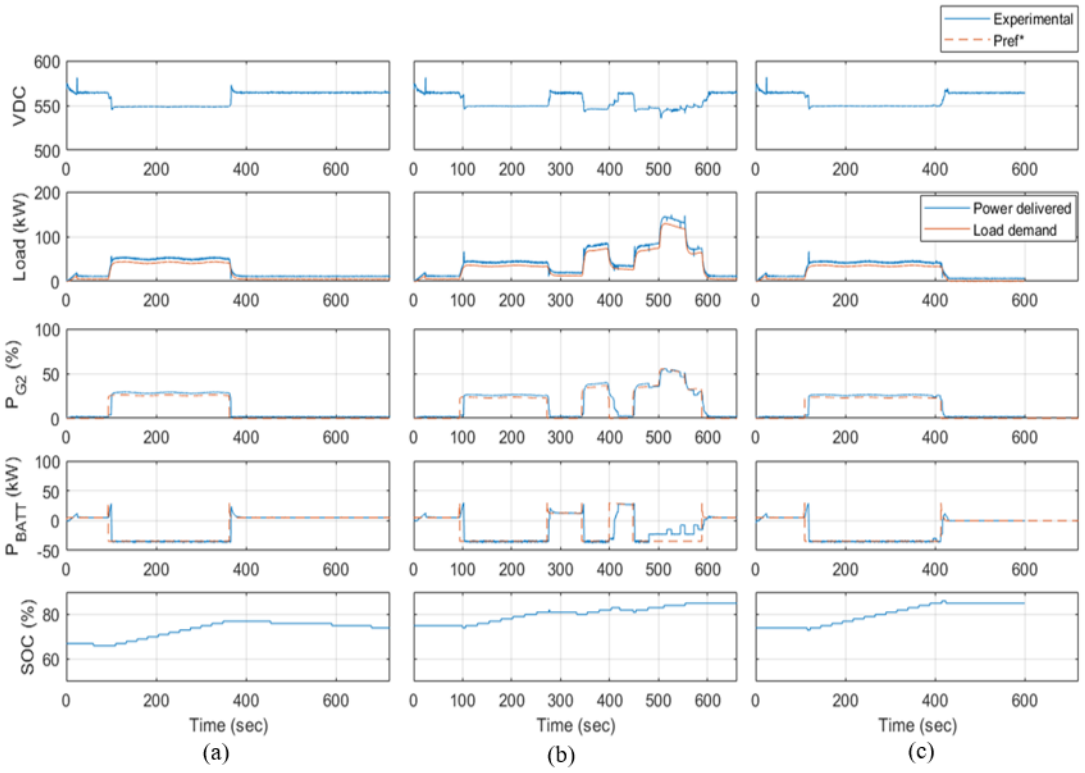

FIGURE 15. Experimental results of improved rule-based approach in (a) Segment 1 (b) Segment 2 (c) Segment 3.

TABLE 6. Specifications of equipment in MARINTEK laboratory full-scale set up.

Equipment	Specifications
Diesel engine 1 (Perkins 1306C)	209kWb, 1500rpm
Diesel engine 2 (Perkins 2506C)	412kWb, 1500rpm
Generator 1	230kVA, 50Hz, 4 poles, 1500rpm
Generator 2	400kVA, 50Hz, 4poles, 1500rpm
Li-ion battery	65Ah, 346V, Peak charging/discharging: 200A/400A, Maximum continuous charging/discharging: 100A/200A
Electric motor	160kW, 50Hz, 4 poles

the whole operation. Segment 1 from 0-12 minutes of the cycle consisting of transit and standby operations, segment 2 from 12-23 minutes of the cycle consisting of transit, short standby and ship assist operations, and segment 3 from 23-35 minutes of the cycle consisting of mainly transit. Due to certain limitations on the lab setup, the experimental procedure is modified to allow manual start of genset, while minimizing the impact on the results. At the start of each segment, the number of required gensets pre-determined from simulation is switched on, and remained online throughout the segment. The performance of the proposed framework with both improved rule-based and ECMS are investigated under a maximum propulsion of 150kW. The experimental results are shown in Fig. 15 and 16.

B. RESULTS AND DISCUSSIONS

The proposed framework is successfully implemented as shown in the results in Fig. 15 and 16. Firstly, the voltage on the DC grid is well maintained between 540-580Vdc, within 6% of voltage droop. One main attribute to the stable voltage is that genset 2 is online throughout the operation cycle, which maintained the DC grid voltage through voltage droop control in the PEMS. Secondly, the power references from the supervisory power management strategies are achieved in the actual power split between the power sources in experimental results. The battery power reference is achieved by operating the bi-directional dc-dc converter in power control mode throughout the cycle. Genset 2 provides the remaining required power in the system, which coincides with the generator power reference. It is observed that the total power delivered to the load is slightly lower than the total power delivered by the power sources, due to power transmission losses in the system. Lastly, the SOC of the battery is well kept within the SOC limit of 30% to 90%.

Comparing the performance of ECMS against the improved rule-based strategy, both strategies show similar performances in segment 1. The advantage of ECMS over Improved Rule-based Strategy is shown in segment 2 and 3. In segment 2, genset 2 is used to provide the required power from the load, as well as charging the battery in the transiting period, based on improved rule-based strategy. ECMS in this case, utilizes available battery power during this transiting

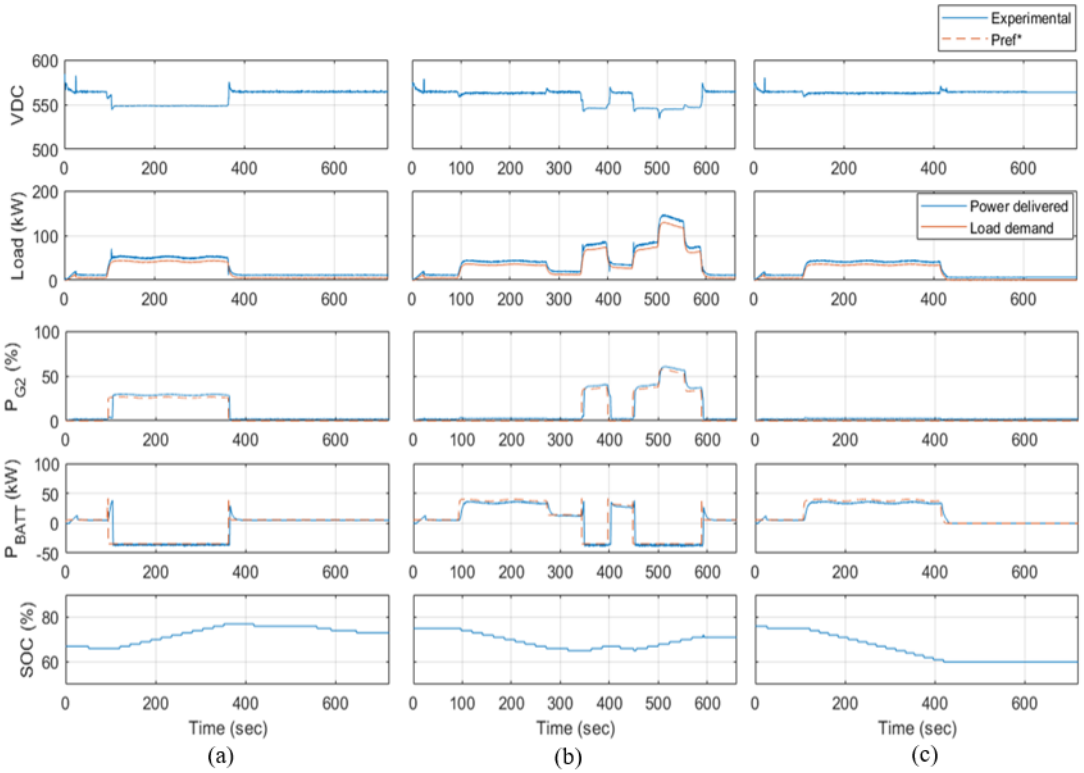

FIGURE 16. Experimental results of ECMS approach in (a) Segment 1 (b) Segment 2 (c) Segment 3.

period, since the SOC of the battery is within the SOC limit. Subsequently, as the load demand during ship assist operation is higher than the maximum discharge power of the battery, both ECMS and rule-based strategy utilizes genset 2 to supply for the load demand. However, since the load demand is lower than the optimal operating region of the engine, loading is increased by charging the battery, to avoid low engine loading. In segment 3, where the load demand is similar to the transiting period in segment 2, same trend is observed where improved rule-based utilizes both genset 2 and battery to provide power for the load, while ECMS utilizes the available battery power. This resulted in a substantial amount of fuel savings in ECMS as compared to rule-based strategy, as shown in Table 7. Since the combined installed power of genset 2 and battery is sufficient for 100% of the maximum propulsion power, genset 1 is not utilized throughout the operation, hence there are no trends of genset 1 in the results in Fig. 15 and 16. Although battery power is used mainly to supply the total load demand for segment 3, a portion of fuel consumption is recorded due to genset 2 in idle mode since it is switched on at the start of the segment, which is a limitation in this experiment. However, both strategies experience the same limitation and are on the same ground of comparison.

Overall, the ECMS demonstrates better fuel efficiency as compared to improved rule-based strategy. The battery seems to be more well-utilized in the case of ECMS in segment 2 and 3, with a net loss of 13% in SOC that contributes to the total fuel savings. In the case where shore charging is possible, this amount of battery energy used can be charged from shore power, which further saves on fuel consumption. The fuel savings achieved from ECMS in this case, can be up to 24.4% with the availability of shore charging. In addition to fuel efficiency, the added advantages of the proposed ECMS strategy against rule-based methods are also validated, where it is able to show consistency in demonstrating more optimal performance when system parameters and load conditions are changed.

TABLE 7. Comparison of fuel consumption and SOC from experimental results.

Segment	PMS	Fuel [kg]	%Savings	$\triangle SOC$
Segment 1	Improved RB	1.833	-	0.07
	ECMS	1.833	0	0.07
Segment 2	Improved RB	2.629	-	0.1
	ECMS	2.131	18.9	-0.04
Segment 3	Improved RB	1.674	-	0.11
	ECMS	0.675	59.7	-0.16
Total	Improved RB	6.136	-	0.28
	ECMS	4.639	24.4	-0.13

V. CONCLUSION AND FUTURE WORK

In this work, the real-time implementation and performance of proposed ECMS approach on actual all-electric hybrid power system have been investigated. Firstly, the dynamic

models of all-electric hybrid power system have been validated on the laboratory-scaled hybrid power system test bed. The validated models have shown that they can be easily re-configured for different system configurations of gensets and batteries, and can be used as a platform for power management studies to analyse the system's response, before real-time implementation on actual all-electric hybrid power system. Secondly, the feasibility of the proposed ECMS power management framework has been demonstrated in real-time on the full-scale experimental set-up identical to an all-electric hybrid tugboat power system, which has laid a foundation for the integration of advance power management strategies to existing power management control system. Finally, the proposed ECMS approach has demonstrated substantial fuel savings and additional advantages over rule-based method. Through the experimental validations, it has been observed that the performance of the rule-based strategy largely depends on the decision factors that are designed based on past experiences or knowledge, which may not guarantee optimal performance when system parameters or loading scenarios changes. Whereas, the proposed ECMS approach can better adapt to different loading scenarios and system configurations, as proven from the full-scale experimental results where ECMS demonstrates significant fuel savings over rule-based method under a different set of system parameters and loading conditions. In addition, it has been shown that rule-based method works according to pre-defined rules for each loading scenario, hence the complexity of designing the rule-based logic will be expected to increase with additional power sources. Whereas ECMS has been designed to cater to different number of power sources, making it easily adaptable to different system configurations where more power sources are considered. Therefore, in real world application with different configurations of hybrid power sources, unknown load conditions and changing system parameters on different system, the proposed ECMS approach has shown to be a potential solution to optimize performance under these changing conditions.

Future work can look into enhancement of the proposed ECMS approach to consider emission cost, investigates in the effects on fuel consumption while minimizing emission, and balance possible trade off between emission and fuel consumption. In addition, power management optimization problem can be extended to primary level controls to further ensures the system reliability in addition to sustainability aspects of fuel and emission savings, taking into consideration potential problems of the DC power distribution system such as constant power instabilities caused by converters operations [33].

ACKNOWLEDGEMENT

The authors would like to thank Kjartan Øye, Kristoffer Dønnestad, Håvard knappskog, Espen Stubberød Olsen and team from ABB AS for the arrangements and technical support at MARINTEK laboratory facilities.

REFERENCES

[1] A. K. Ådnanes, "Reduction of fuel consumption and environmental footprint for ships, using electric or hybrid propulsion," presented at the WMTC 2009. [Online]. Available: http://imare.in/media/30639/paper-no-5a-3-dr-akadnanes.pdf

[2] T. Jaster, A. Rowe, and Z. Dong, "Modeling and simulation of a hybrid electric propulsion system of a green ship," in *Proc. IEEE/ASME 10th Int. Conf. Mechatronic Embedded Syst. Appl. (MESA)*, Sep. 2014, pp. 1–6.

[3] J. Hou, J. Sun, and H. F. Hofmann, "Mitigating power fluctuations in electric ship propulsion with hybrid energy storage system: Design and analysis," *IEEE J. Oceanic Eng.*, vol. 43, no. 1, pp. 93–107, Jan. 2018.

[4] J. Han, J. F. Charpentier, and T. Tang, "An energy management system of a fuel cell/battery hybrid boat," *Energies*, vol. 7, no. 5, pp. 2799–2820, 2014.

[5] M. R. Miyazaki, A. J. Sørensen, N. Lefebvre, K. K. Yum, and E. Pedersen, "Hybrid modeling of strategic loading of a marine hybrid power plant with experimental validation," *IEEE Access*, vol. 4, pp. 8793–8804, 2016.

[6] J. O. Lindtjorn, F. Wendt, B. Gundersen, and J. F. Hansen, "Demonstrating the benefits of advanced power systems and energy storage for DP vessels," in *Proc. Dyn. Positioning Conf.*, 2014, pp. 1–24.

[7] K. K. Tafanidis, K. D. Taxeidis, G. J. Tsekouras, and F. D. Kanellos, "Optimal operation of war-ship electric power system equipped with energy storage system," *J. Comput. Model.*, vol. 3, no. 4, pp. 41–60, 2013.

[8] R. D. Geertsma, R. R. Negenborn, K. Visser, and J. J. Hopman, "Design and control of hybrid power and propulsion systems for smart ships: A review of developments," *Appl. Energy*, vol. 194, pp. 30–54, May 2017.

[9] M. R. Miyazaki, A. J. Sørensen, and B. J. Vartdal, "Reduction of fuel consumption on hybrid marine power plants by strategic loading with energy storage devices," *IEEE Power Energy Technol. Syst. J.*, vol. 3, no. 4, pp. 207–217, Dec. 2016.

[10] M. Kalikatzarakis, R. D. Geertsma, E. J. Boonen, K. Visser, and R. R. Negenborn, "Ship energy management for hybrid propulsion and power supply with shore charging," *Control Eng. Pract.*, vol. 76, pp. 133–154, Jul. 2018.

[11] G. Seenumani, J. Sun, and H. Peng, "A numerically efficient iterative procedure for hybrid power system optimization using sensitivity functions," in *Proc. Amer. Control Conf. (ACC)*, Jul. 2007, pp. 4738–4743.

[12] G. Seenumani, J. Sun, and H. Peng, "Real-time power management of integrated power systems in all electric ships leveraging multi time scale property," *IEEE Trans. Control Syst. Technol.*, vol. 20, no. 1, pp. 232–240, Jan. 2012.

[13] G. Seenumani, J. Sun, and H. Peng, "A hierarchical optimal control strategy for power management of hybrid power systems in all electric ships applications," in *Proc. 49th IEEE Conf. Decis. Control (CDC)*, Dec. 2010, pp. 3972–3977.

[14] T. Van Vu, D. Gonsoulin, F. Diaz, C. S. Edrington, and T. El-Mezyani, "Predictive control for energy management in ship power systems under high-power ramp rate loads," *IEEE Trans. Energy Convers.*, vol. 32, no. 2, pp. 788–797, Jun. 2017.

[15] H. Park *et al.*, "Real-time model predictive control for shipboard power management using the IPA-SQP approach," *IEEE Trans. Control Syst. Technol.*, vol. 23, no. 6, pp. 2129–2143, Nov. 2015.

[16] T. I. Bø and T. A. Johansen, "Battery power smoothing control in a marine electric power plant using nonlinear model predictive control," *IEEE Trans. Control Syst. Technol.*, vol. 25, no. 4, pp. 1449–1456, Jul. 2017.

[17] B. Zahedi, L. E. Norum, and K. B. Ludvigsen, "Optimized efficiency of all-electric ships by dc hybrid power systems," *J. Power Sour.*, vol. 255, pp. 341–354, Jun. 2014.

[18] T. L. Vu, A. A. Ayu, J. S. Dhupia, L. Kennedy, and A. K. Adnanes, "Power management for electric tugboats through operating load estimation," *IEEE Trans. Control Syst. Technol.*, vol. 23, no. 6, pp. 2375–2382, Nov. 2015.

[19] E. K. Dedes, "Investigation of hybrid systems for diesel powered ships," Ph.D. dissertation, Fac. Eng. Environ., Univ. Southampton, Southampton, U.K., 2013.

[20] E. K. Dedes, D. A. Hudson, and S. R. Turnock, "Investigation of diesel hybrid systems for fuel oil reduction in slow speed ocean going ships," *Energy*, vol. 114, pp. 444–456, Nov. 2016.

[21] L. W. Y. Chua, T. Tjahjowidodo, G. L. Seet, R. Chan, and A. K. Adnanes, "Equivalent consumption minimization strategy for hybrid all-electric tugboats to optimize fuel savings," in *Proc. Amer. Control Conf. (ACC)*, Boston, MA, USA, 2016, pp. 6803–6808.

[22] R. Chan, L. W. Y. Chua, and T. Tjahjowidodo, "Enabling technologies for sustainable all—Electric hybrid vessels (invited paper)," in *Proc. IEEE Int. Conf. Sustain. Energy Technol. (ICSET)*, Hanoi, Vietnam, Nov. 2016, pp. 401–406.
[23] L. Kennedy, J. Soong, and J. O. Lindtjorn, "All-electric hybrid propulsion for the next generation of tugboats," in *Proc. Tugnol.*, London, U.K., 2013.
[24] F. D. Kanellos, G. J. Tsekouras, and J. Prousalidis, "Onboard DC grid employing smart grid technology: Challenges, state of the art and future prospects," *IET Elect. Syst. Transp.*, vol. 5, no. 1, pp. 1–11, Mar. 2015.
[25] *DS1103 PPC Controller Board: Hardware Installation and Configuration For Release 2013-B*, dSPACE GmbH, Paderborn, Germany, 2013,
[26] B. Zahedi and L. E. Norum, "Modelling and simulation of hybrid electric ships with DC distribution systems," in *Proc. 15th Eur. Conf. Power Electron. Appl. (EPE)*, Sep. 2013, pp. 1–10.
[27] T. H. Syverud, "Modeling and control of a DC-grid hybrid power system with battery and variable speed diesel generators," M.S. thesis, Dept. Electr. Power Eng., Norwegian Univ. Sci. Technol., Trondheim, Norway, 2016.
[28] O. Tremblay and L.-A. Dessaint, "Experimental validation of a battery dynamic model for EV applications," *World Electr. Veh. J.*, vol. 3, pp. 289–298, May 2009.
[29] S. N. Motapon, L.-A. Dessaint, and K. Al-Haddad, "A comparative study of energy management schemes for a fuel-cell hybrid emergency power system of more-electric aircraft," *IEEE Trans. Ind. Electron.*, vol. 61, no. 3, pp. 1320–1334, Mar. 2014.
[30] J. F. Hansen, "Modelling and control of marine power systems," Ph.D. dissertation, Dept. Marine Technol., Norwegian Univ. Sci. Technol., Trondheim, Norway, 2000.
[31] B. Zahedi and L. E. Norum, "Voltage regulation and power sharing control in ship LVDC power distribution systems," in *Proc. 15th Eur. Conf. Power Electron. Appl. (EPE)*, Sep. 2013, pp. 1–8.
[32] G. Paganelli, S. Delprat, T. M. Guerra, J. Rimaux, and J. J. Santin, "Equivalent consumption minimization strategy for parallel hybrid powertrains," in *Proc. IEEE 55th Veh. Technol. Conf. (VTC)*, vol. 4, May 2002, pp. 2076–2081.
[33] E. Hossain, R. Perez, A. Nasiri, and S. Padmanaban, "A comprehensive review on constant power loads compensation techniques," *IEEE Access*, vol. 6, pp. 33285–33305, 2018.

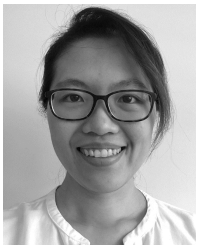

LIZA W. Y. CHUA received the bachelor's degree from Nanyang Technological University, Singapore, in 2013, where she is currently pursuing the Ph.D. with the School of Mechanical and Aerospace Engineering. Her research is in collaboration with ABB. Pte. Ltd., as a part of the Industrial Postgraduate Programme sponsored by the Singapore Economic Development Board. Her research interests include the control and optimization of marine hybrid power systems.

TEGOEH TJAHJOWIDODO received the Ph.D. degree from Katholieke Universiteit Leuven, Belgium, in 2006. He joined the Flanders' Mechatronics Technology Center, Belgium, a research center in the mechatronics area, where he was involved in several projects, mainly in nonlinear dynamics. He is currently an Associate Professor and an Assistant Chair of research at the School of Mechanical and Aerospace Engineering, Nanyang Technological University, Singapore. His research interests are in nonlinear dynamics, modeling, identification, and control.

GERALD G. L. SEET received the Ph.D. degree from Aston University, U.K., in 1985. He is currently an Associate Professor with the School of Mechanical and Aerospace Engineering, Nanyang Technological University, Singapore. His main research interests are in mechatronics and field robotics, with specific interest in underwater mobile robotics, fluid power systems, as well as unmanned aerial vehicles, and collaborative robotic systems.

RICKY CHAN received the Ph.D. degree in electrical engineering from Purdue University, USA, in 2009. Following graduation, he has held a number of positions in R&D with A*STAR and Rolls-Royce Singapore, before joining ABB in 2014. He is currently the Technology Manager of ABB Marine & Ports, Helsinki, Finland, where he leads a team of specialists in the development of advanced electric solutions for marine applications.